

---

# Beyond Normalization: Rethinking the Partition Function as a Difficulty Scheduler for RLVR

---

Dohyung Kim<sup>1</sup> Minbeom Kim<sup>1</sup> Jeonghye Kim<sup>2</sup> Sangmook Lee<sup>1</sup> Sojeong Rhee<sup>2</sup> Kyomin Jung<sup>1</sup>

## Abstract

Reward-maximizing RL methods enhance the reasoning performance of LLMs, but often reduce the diversity among outputs. Recent works address this issue by adopting GFlowNets, training LLMs to match a target distribution while jointly learning its partition function. In contrast to prior works that treat this partition function solely as a normalizer, we reinterpret it as a per-prompt expected-reward (i.e., online accuracy) signal, leveraging this unused information to improve sample efficiency. Specifically, we first establish a theoretical relationship between the partition function and per-prompt accuracy estimates. Building on this key insight, we propose **Partition Function-Guided RL** (PACED-RL), a post-training framework that leverages accuracy estimates to prioritize informative question prompts during training, and further improves sample efficiency through an accuracy estimate error-prioritized replay. Crucially, both components reuse information already produced during GFlowNet training, effectively amortizing the compute overhead into the existing optimization process. Extensive experiments across diverse benchmarks demonstrate strong performance improvements over GRPO and prior GFlowNet approaches, highlighting PACED-RL as a promising direction for a more sample efficient distribution-matching training for LLMs.

## 1. Introduction

Reinforcement Learning (RL) has emerged as a cornerstone for improving the reasoning performance of Large Language Models (LLMs) (Jaech et al., 2024; Guo et al., 2025; Comanici et al., 2025). By enabling models to repeatedly self-explore and maximize the expected reward, such methods

<sup>1</sup>Seoul National University <sup>2</sup>KAIST. Correspondence to: Dohyung Kim <kimdohyung@snu.ac.kr>, Kyomin Jung <kjung@snu.ac.kr>.

have been shown to significantly enhance complex reasoning performances (Shao et al., 2024; Yu et al., 2025b).

Despite these gains, *reward-maximizing* RL methods such as PPO (Schulman et al., 2017) and GRPO (Shao et al., 2024) often lead to an overly sharpened output distribution (Huang et al., 2025; Li et al., 2025c), leading to limited diversity among generated outputs (Padmakumar & He, 2024; Shypula et al., 2025). In the context of RL post-training for LLM reasoning, however, preserving diversity is essential for a thorough exploration of the search space, enabling the discovery of diverse valid reasoning strategies and the effective application of inference-time techniques (Yue et al., 2025; Li et al., 2025b; Chen et al., 2025).

To alleviate this issue, recent methods such as FlowRL (Zhu et al., 2025a) depart from direct reward maximization and instead employ GFlowNets (Bengio et al., 2023), focusing on reward *distribution matching*. Unlike post-training with reward-maximizing RL, where the LLM policy is optimized to maximize the expected reward, FlowRL trains the policy to match a reward-induced target distribution, with a partition function jointly learned as the normalizer of that target reward distribution. At optimum, this partition function corresponds to the sum of the reward-induced distribution mass, accumulated over all possible completions for a given input question prompt. By explicitly modeling the target distribution and pushing the policy toward it, this distributional objective encourages mode coverage, thus mitigating the diversity limitations of conventional RL methods.

In this work, we revisit the GFlowNet partition function used in LLM post-training. We show that the partition function—previously regarded only as a necessary overhead for target distribution normalization and training stability—naturally encodes per-prompt online accuracy information that can be leveraged for significant improvements in sample efficiency. Specifically, we establish a theoretical connection between the partition function and online accuracies, showing that it can be used directly to estimate the accuracy of a given question prompt under the policy during training. This insight allows us to re-purpose the cost already incurred by GFlowNet training to guide adaptive prompt selection and replay prioritization, focusing on the most informative training samples at each step.

Building on this observation, we propose **Partition Function-Guided RL** (PACED-RL), a novel GFlowNet-based LLM post-training framework that extends the role of the partition function beyond normalization to enable a more sample efficient training, while preserving the inherent diversity benefits of GFlowNets. By making use of the partition function to directly predict accuracy estimates, our method performs difficulty-aware adaptive prompt selection, sampling question prompts that maximize learning efficiency at each step. Furthermore, inspired by prior work on replay mechanisms (Schaul et al., 2015; Shen et al., 2023; Kim et al., 2024), we introduce an accuracy estimation error-prioritized replay strategy that exploits the off-policy tolerance of the GFlowNet objective to further boost sample efficiency. Crucially, both components reuse information *already* produced during standard GFlowNet training, effectively amortizing the cost of adaptive prompt selection and replay prioritization into the existing optimization process.

Extensive experiments across mathematical reasoning and coding benchmarks showcase the effectiveness of PACED-RL. On AIME benchmarks, PACED-RL improves average pass@1 performance by up to 29.1% and 40.0% over GRPO and FlowRL, respectively. Moreover, on the pass@ $k$  metric, which we employ as a proxy for diversity and exploration capacity (Li et al., 2025b; Zhu et al., 2025b), PACED-RL achieves consistent improvements over baselines, outperforming GRPO and FlowRL by up to 14.2% and 9.1%.

Our main results and key contributions are as follows:

- We theoretically show that the GFlowNet partition function for LLM post-training is linked to online accuracies, enabling it to directly serve as online accuracy estimates.
- We introduce PACED-RL, which leverages these accuracy estimates to perform difficulty-aware adaptive prompt selection and estimation-error-prioritized replay, boosting training efficiency while preserving output diversity.
- We carry out extensive evaluations across code generation and mathematical reasoning benchmarks, and show that PACED-RL achieves clear performance gains over various RLVR baselines.

Overall, our results show that PACED-RL offers a principled and practical way to further enhance distribution-matching training of LLMs for reasoning tasks.

## 2. Preliminaries

### 2.1. Reinforcement Learning with Verifiable Rewards

Reinforcement Learning with Verifiable Rewards (RLVR) has emerged as an effective approach for training LLMs on verifiable tasks. Given an output  $\mathbf{y}$  generated by an LLM policy  $\pi_\theta$  for an input question prompt  $\mathbf{x}$  sampled from a dataset  $\mathcal{D}$ , a deterministic reward function  $r(\mathbf{x}, \mathbf{y}) \in \{0, 1\}$

assigns a binary score to  $\mathbf{y}$  by assessing its correctness. RLVR optimizes the following KL-regularized objective:

$$\max_{\theta} \mathbb{E}_{\substack{\mathbf{x} \sim \mathcal{D} \\ \mathbf{y} \sim \pi_\theta(\cdot | \mathbf{x})}} [r(\mathbf{x}, \mathbf{y})] - \beta D_{\text{KL}}(\pi_\theta(\cdot | \mathbf{x}) \| \pi_{\text{ref}}(\cdot | \mathbf{x})) \quad (1)$$

, where  $\pi_{\text{ref}}$  denotes the untrained base reference model and  $\beta$  denotes the KL divergence regularization coefficient.

In particular, the optimal policy for Eq. 1 admits a closed-form solution, expressed as:

$$\pi^*(\mathbf{y} | \mathbf{x}) = \frac{\pi_{\text{ref}}(\mathbf{y} | \mathbf{x}) \exp(\beta^{-1}r(\mathbf{x}, \mathbf{y}))}{Z(\mathbf{x})}. \quad (2)$$

Here,  $Z(\mathbf{x})$  denotes the intractable partition function that normalizes the distribution by summing over all possible outputs  $\mathbf{y}$  for a given question prompt  $\mathbf{x}$ :

$$Z(\mathbf{x}) = \sum_{\mathbf{y}} \pi_{\text{ref}}(\mathbf{y} | \mathbf{x}) \exp(\beta^{-1}r(\mathbf{x}, \mathbf{y})). \quad (3)$$

### 2.2. GFlowNets for LLM Post-Training

GFlowNets train a policy  $\pi_\theta$  to sample diverse discrete, compositional objects in proportion to an unnormalized target reward *distribution*  $R(\mathbf{x}, \mathbf{y})$ . In the RLVR setting, this objective biases the policy to sample high-reward outputs  $\mathbf{y}$  (correct solutions) rather than low-reward outputs (incorrect solutions) for a given input question prompt  $\mathbf{x}$ .

To train an LLM policy  $\pi_\theta$  to sample from the optimal policy in Eq. 2 using GFlowNet objectives, previous works (Lee et al., 2025; Zhu et al., 2025a) configure the unnormalized reward distribution as  $R(\mathbf{x}, \mathbf{y}) = \pi_{\text{ref}}(\mathbf{y} | \mathbf{x}) \exp(\beta^{-1}r(\mathbf{x}, \mathbf{y}))$ , and train a learnable  $Z_\phi(\mathbf{x})$ , which approximates the intractable partition function  $Z(\mathbf{x})$  in Eq. 3. By explicitly modeling the target distribution and its normalization through a learnable partition function, GFlowNets reduce policy learning to matching this target distribution.

Plugging this  $R(\mathbf{x}, \mathbf{y})$  and  $Z_\phi(\mathbf{x})$  into the Trajectory Balance (TB) objective (Malkin et al., 2022) for GFlowNet training leads to the loss function defined as follows:

$$\mathcal{L}_{\text{TB}}(\mathbf{x}, \mathbf{y}; \theta, \phi) = \left[ \log \left( \frac{Z_\phi(\mathbf{x}) \pi_\theta(\mathbf{y} | \mathbf{x})}{\pi_{\text{ref}}(\mathbf{y} | \mathbf{x}) \exp(\beta^{-1}r(\mathbf{x}, \mathbf{y}))} \right) \right]^2. \quad (4)$$

Minimizing this TB loss is equivalent, in terms of expected gradients, to minimizing the KL divergence between  $\pi_\theta$  and the optimal policy in Eq. 2, with the intractable partition function approximated by  $Z_\phi(\mathbf{x})$  (Zhu et al., 2025a):

$$\begin{aligned} \min_{\theta} \mathcal{L}_{\text{TB}}(\mathbf{x}, \mathbf{y}; \theta, \phi) &\iff \\ \min_{\theta} D_{\text{KL}} \left( \pi_\theta(\mathbf{y} | \mathbf{x}) \left\| \frac{\pi_{\text{ref}}(\mathbf{y} | \mathbf{x}) \exp(\beta^{-1}r(\mathbf{x}, \mathbf{y}))}{Z_\phi(\mathbf{x})} \right. \right) \end{aligned} \quad (5)$$

Thus,  $\mathcal{L}_{\text{TB}}$  drives the LLM policy  $\pi_\theta$  to sample from the optimal policy, while simultaneously training  $Z_\phi(\mathbf{x})$  to normalize the unnormalized target reward distribution  $\pi_{\text{ref}}(\mathbf{y} \mid \mathbf{x}) \exp(\beta^{-1} r(\mathbf{x}, \mathbf{y}))$ .

### 3. Related Works

#### 3.1. GFlowNets for LLM Post-Training

In the context of LLM post-training, GFlowNets have been adapted for domains such as preference alignment, red-teaming, and reasoning (Kwon et al., 2024; Lee et al., 2025; Yu et al., 2025a; Zhu et al., 2025a). Bartoldson et al. (2025) further proposes an asynchronous, distributed RL pipeline for LLMs that leverages GFlowNets for better throughput.

Despite their success, existing GFlowNet-based methods for LLM post-training primarily treat the partition function as a necessary normalization variable required to define the target distribution. While several works study improved optimization techniques for GFlowNets, such as replacing the learned  $Z_\phi(\mathbf{x})$  with a batch-estimate (Zhang et al., 2023; Bartoldson et al., 2025), the information encoded in  $Z_\phi(\mathbf{x})$  has not been exploited beyond normalization.

Most closely related to our work is FlowRL (Zhu et al., 2025a). FlowRL adapts GFlowNets to the synchronous RL setting, where training alternates between the rollout generation phase and the optimization phase, with added stability techniques suited for RLVR. Our work extends prior works in GFlowNets for LLM post-training by reformulating  $Z_\phi(\mathbf{x})$  for online accuracy estimation, enabling adaptive prompt selection and replay strategies that enhance sample efficiency without incurring additional cost.

#### 3.2. Adaptive Prompt Selection for RLVR

Recent works show that training on question prompts of intermediate difficulty—those achieving approximately 0.5 accuracy with respect to the policy—improves sample efficiency in the RLVR setting (Bae et al., 2025; Foster et al., 2025). Building on this observation, adaptive prompt selection methods that selectively sample such prompts for training have emerged as a promising direction for improved sample efficiency. Crucially, to effectively enable such methods, obtaining reliable online accuracy estimates is needed.

Recent works such as Yu et al. (2025b); Foster et al. (2025); Zhang et al. (2025) over-sample a pool of question prompts larger than the training batch at each step, and filter out less informative prompts based on the observed accuracies after the rollout generation phase. Though effective, such approaches lead to a significantly increased number of rollout generation, substantially increasing computational overhead. An alternative line of work maintains per-question accuracy histories, and estimates online accuracies via Bayesian pos-

terior estimation or probabilistic filtering (Zheng et al., 2025; Qu et al., 2025; Zeng et al., 2025), enabling lightweight prompt selection. However, on large datasets, these estimates can suffer from off-policy bias: over the course of an epoch, the policy may improve substantially, rendering the accuracy estimates stale when revisited.

Distinct from previous approaches, our work reuses the partition function inherent to GFlowNets for online accuracy estimation, eliminating the need for employing such auxiliary mechanisms to guide adaptive prompt selection.

#### 3.3. Prioritized Experience Replay

Replay is widely adopted in RL training, owing to its efficacy in enhancing sample efficiency. To further enhance replay effectiveness, Schaul et al. (2015) propose Prioritized Experience Replay (PER) for Q-learning, which prioritizes samples with large temporal-difference errors, allowing the policy to focus learning on more informative data. Building on this idea, numerous PER variants (Horgan et al., 2018; Hessel et al., 2018; Sujit et al., 2023) have been developed to improve training stability and data efficiency.

Replay mechanisms have also been extensively adopted in the GFlowNets literature (Shen et al., 2023; Kim et al., 2024; Bartoldson et al., 2025), where the training objective naturally accommodates off-policy data, and more recently, have been explored in the RLVR setting (Wang et al., 2025b; Li et al., 2025a). A recurring insight across both domains is that prioritizing high-reward and more recent samples improves the effectiveness of the replay. Extending upon previous works, our work tailors prioritization to improve partition function learning and sample efficiency by leveraging its connection to accuracy estimates and prioritizing samples with large accuracy estimation errors.

### 4. PACED-RL

We begin by revisiting the role of the GFlowNet partition function for LLM post-training. While the learnable partition function  $Z_\phi$  is typically introduced as a necessary normalization term, we reveal that it in fact encodes meaningful information about per-question online accuracies. Specifically, we first show that for a question  $\mathbf{x}$ ,  $Z_\phi$  provides an estimate of the accuracy  $p_{\text{old}}(\mathbf{x})$ . Here,  $p_{\text{old}}(\mathbf{x})$  denotes the accuracy for  $\mathbf{x}$  under the pre-update policy  $\pi_{\text{old}}$ , the policy from which rollouts are sampled at each step. We then show how these accuracy estimates can be leveraged to improve sample efficiency by focusing on the most informative samples throughout the training process.

#### 4.1. Partition Function and Online Accuracy Estimates

Under a Trajectory Balance loss modified from Eq. 4, we show that the optimal partition function admits a direct rela-

tionship to per-question online accuracy estimates. Specifically, we replace  $\pi_{\text{ref}}$  with  $\pi_{\text{old}}$ :

$$\mathcal{L}_{\text{ours}}(\mathbf{x}, \mathbf{y}; \theta, \phi) = \left[ \log \left( \frac{Z_\phi(\mathbf{x}) \pi_\theta(\mathbf{y} | \mathbf{x})}{\pi_{\text{old}}(\mathbf{y} | \mathbf{x}) \exp(\beta^{-1} r(\mathbf{x}, \mathbf{y}))} \right) \right]^2. \quad (6)$$

Replacing the reference policy  $\pi_{\text{ref}}$  with  $\pi_{\text{old}}$  yields an interpretation as training to sample from the optimal policy of a KL-regularized objective (Eq. 1), with the KL divergence regularization anchored at  $\pi_{\text{old}}$  rather than  $\pi_{\text{ref}}$ .

**Proposition 4.1.** *Given  $Z^*(\mathbf{x})$ , the optimal partition function, we can express  $p_{\text{old}}(\mathbf{x})$  as follows:*

$$p_{\text{old}}(\mathbf{x}) = \beta \log Z^*(\mathbf{x}) - \beta D_{\text{KL}}(\pi_{\text{old}}(\cdot | \mathbf{x}) \| \pi_\theta(\cdot | \mathbf{x})). \quad (7)$$

The detailed derivations are provided in Appendix A. Proposition 4.1 reveals that the partition function, previously used solely for the normalization of the target distribution, can be directly interpreted as an online accuracy signal. Importantly, this information is already produced as part of the GFlowNet training, incurring no extra computational cost.

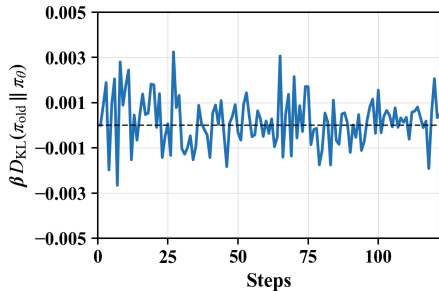


Figure 1. Training dynamics of mean of estimated values of  $\beta D_{\text{KL}}(\pi_{\text{old}}(\cdot | \mathbf{x}) \| \pi_\theta(\cdot | \mathbf{x}))$  of Qwen2.5-Math-1.5B trained on the DeepScaleR dataset, using the TB loss defined in Eq. 6

## 4.2. Obtaining Practical Online Accuracy Estimates

Ideally, the accuracy estimate for  $\mathbf{x}$  should be obtainable as a function of  $\mathbf{x}$  without requiring additional computation. While Eq. 7 provides theoretical insight, it does not immediately yield a practical online accuracy estimate from  $Z_\phi$ , as KL divergence between policies is typically estimated using expensive Monte Carlo rollouts (Schulman et al., 2015). Below, we show that the KL term in Eq. 7 remains uniformly small during training and can therefore be safely omitted, yielding a simple accuracy estimator dependent only on  $Z_\phi$ .

In practice, standard training practices—such as small learning rates and gradient norm clipping—generally ensure that parameter updates remain small. As KL divergence admits a second-order approximation that scales quadratically with the parameter update (Achiam et al., 2017; Martens, 2020), small parameter updates typically lead to a controlled KL divergence between successive policies.

As shown in Fig. 1, the empirically estimated mean values of  $\beta D_{\text{KL}}(\pi_{\text{old}}(\cdot | \mathbf{x}) \| \pi_\theta(\cdot | \mathbf{x}))$  remains uniformly small over the course of training, with the maximum absolute value remaining below  $4 \times 10^{-3}$ . Since the range of online accuracies  $p_{\text{old}}(\mathbf{x})$  is  $[0, 1]$  due to the 0/1 binary reward setting, the error that would be introduced by discarding the KL divergence term is small at the scale relevant for difficulty-aware prompt selection.

Motivated by this observation, we obtain a practical, biased estimator by discarding the KL divergence term in Eq. 7:

$$p_{\text{old}}(\mathbf{x}) \approx \beta \log Z^*(\mathbf{x}) \quad (8)$$

and train  $Z_\phi(\mathbf{x})$ , which approximates the optimal  $Z^*(\mathbf{x})$ . While this approximation introduces an empirically stable and controlled bias into the accuracy estimates, it enables per-question online accuracy estimation without auxiliary estimators or additional rollouts. Consequently, the cost of accuracy estimation is effectively amortized into the existing GFlowNet training process.

## 4.3. Adaptive Prompt Selection Using Online Accuracy Estimates

Having obtained online accuracy estimates directly from  $Z_\phi$  without additional cost, we can naturally integrate adaptive prompt selection into the training pipeline.

Prior work has shown that question prompts of intermediate difficulty provide the most sample-efficient learning signal (Bae et al., 2025; Foster et al., 2025). Leveraging the online accuracy estimates from  $Z_\phi$ , we therefore bias training toward question prompts whose predicted accuracies lie in the vicinity of 0.5, ensuring that the policy consistently focuses on the most informative prompts during training.

Specifically, at training step  $t$ , we begin by utilizing Eq. 8 to obtain  $\{\hat{p}_{\text{old}}(\mathbf{x}_i)\}_{i=1}^{|\mathcal{D}|}$ , the estimates of the online accuracies for question prompts in the dataset. Similar to previous works (Yue et al., 2025; Foster et al., 2025), we then greedily select the top- $m$  questions whose estimated accuracies are closest to the target accuracy  $\tau$ , where  $m$  denotes the training batch size. The selected  $m$  questions are then used for the  $t$ -th training step. While we fix  $\tau$  to 0.5 for optimal sample efficiency in the main experiments, we report results for other configurations of  $\tau$  in Sec. 5.3.

Following the FlowRL pipeline, for each of the  $m$  selected questions, we generate  $N$  rollouts and update both the policy  $\pi_\theta$  and the partition function  $Z_\phi$  by minimizing Eq. 6.

## 4.4. Accuracy Estimation Error-Prioritized Replay

To further improve sample efficiency and the calibration of  $Z_\phi$ , we introduce an accuracy estimation error-prioritized replay strategy. Unlike prior replay prioritization approaches (Schaul et al., 2015; Shen et al., 2023), our method

exploits the connection between  $Z_\phi$  and online accuracy estimates by focusing on samples with large estimation errors. Intuitively, these samples provide the most informative learning signal for  $Z_\phi$ ; this leads to better-calibrated accuracy estimates and a more accurate normalization of the target reward distribution, thereby improving training.

Specifically, we maintain a replay buffer that stores prompt–output pairs  $\{\mathbf{x}, \mathbf{y}\}$ . Following prior findings that replay is most effective with high-reward and recent samples (Bartoldson et al., 2025; Li et al., 2025a), we restrict the buffer to outputs satisfying  $r(\mathbf{x}, \mathbf{y}) = 1$ . Among retained pairs, we prioritize pairs associated with question prompts  $\mathbf{x}$  with the highest accuracy estimation error:

$$\text{priority}(\mathbf{x}) = \left| \frac{N_{\text{correct}}}{N} - \hat{p}_{\text{old}}(\mathbf{x}) \right|, \quad (9)$$

, where  $\frac{N_{\text{correct}}}{N}$  denotes the observed accuracy for question  $\mathbf{x}$  computed from  $N$  rollouts generated by  $\pi_{\text{old}}$  during the rollout generation process of the training pipeline.

We utilize a fixed-capacity replay buffer of size  $B_{\text{max}}$  into which  $B_{\text{add}}$  new samples are added at every training step. This design bounds the age of stored trajectories and thereby controls the degree of off-policyness of the buffer (Fedus et al., 2020). We then augment the training batch with the contents stored in the replay buffer at each training step.

A complete description of our full PACED-RL algorithm, consisting of adaptive prompt selection and accuracy estimate error-prioritized replay, is shown in Algorithm 1.

## 5. Experiments

### 5.1. Experimental Setup

**Datasets & Models.** We conduct experiments in the code generation domain and the mathematical reasoning domain. For code generation, we train on the DeepCoder dataset (Luo et al., 2025a; Zhu et al., 2025a) using the DeepSeek-R1-Distill-Qwen-1.5B model (Guo et al., 2025). For mathematical reasoning, we use the DeepScaleR dataset (Luo et al., 2025b) and adopt Qwen2.5-Math-1.5B and Qwen2.5-Math-7B (Yang et al., 2024) as base models. Across all runs, PACED-RL is trained with  $\beta = 0.05$  and replay buffer capacity  $B_{\text{max}}$  of 128, with  $B_{\text{add}} = 64$  prompt–output pairs added to the buffer at each step. Similar to prior works (Lee et al., 2025; Zhu et al., 2025a), we use a 3-layer MLP stacked on top of frozen, pre-computed reference model embeddings of question prompts  $\mathbf{x}$  to parameterize  $Z_\phi$ .

**Training & Evaluation.** We adopt the widely used verl library (Sheng et al., 2025) for training. Across all runs, we fix the learning rate to 1e-6 and generate 8 rollouts per question prompt, i.e.  $N = 8$ . Due to compute resource constraints, we set the maximum generation length to 3072 tokens for

all runs. For code generation, we evaluate on HumanEval+ (Chen, 2021) and LiveCodeBench (Jain et al., 2025), and report the pass@1 performance averaged over 8 attempts throughout training. For evaluation on the mathematical reasoning domain, we use the MATH500 (Hendrycks et al., 2021), MinervaMath (Lewkowycz et al., 2022), Olympiad-Bench (He et al., 2024), and AIME24/25 benchmarks. Similar to prior works (Wang et al., 2025b; Zheng et al., 2025), we evaluate models every 10 steps and report the pass@1 and pass@ $k$  performance of the checkpoint with the best average performance across benchmarks. Hyperparameters and other implementational details are in Appendix B.

**Baselines.** To comprehensively evaluate PACED-RL, we compare against representative baselines.

**(1) No Adaptive Prompt Selection:** We include **GRPO** and **FlowRL** as standard baselines that sample prompts uniformly from the training dataset. Neither method performs adaptive prompt selection; **GRPO** represents the reward-maximization approach, while **FlowRL** represents the distribution-matching algorithm based on GFlowNets. **(2) With Adaptive Prompt Selection:** We include Dynamic Sampling (**DS**) (Yu et al., 2025b) and **LILO** (Foster et al., 2025) as baselines that perform adaptive prompt selection by over-sampling  $M > m$  question prompts from the dataset at each training step. After generating rollouts for each of the  $M$  over-sampled prompts, DS discards question prompts with observed accuracies of 0 or 1, whereas LILO selects the top- $m$  question prompts whose accuracies are closest to 0.5. We also compare PACED-RL against **MoPPS** (Qu et al., 2025), which estimate prompt accuracies without additional over-sampling. MoPPS maintains per-question prompt accuracy histories and applies Bayesian posterior estimation, selecting the top- $m$  question prompts whose estimated accuracies are closest to 0.5 at each training step.

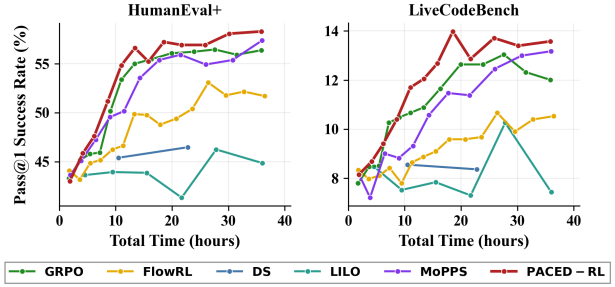


Figure 2. Pass@1(%) dynamics of DeepSeek-R1-Distill-Qwen-1.5B plotted with respect to wall-clock time. Pass@1 values obtained via averaging over 8 independent attempts.

### 5.2. Main Results

**Code Generation.** As shown in Fig. 2, PACED-RL consistently achieves the highest pass@1 performance through-

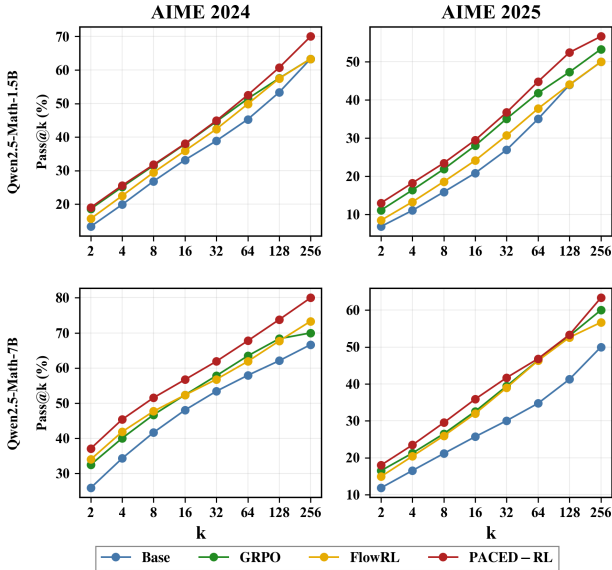


Figure 3. Pass@k(%) curves of Qwen2.5-Math-7B trained on GRPO, FlowRL, and PACED-RL and evaluated on AIME 24 and AIME24 for  $k \in \{2, 4, 8, 16, 32, 64, 128, 256\}$ . Across all evaluated values of  $k$ , PACED-RL achieves the highest performance.

out training compared to all baselines, illustrating the benefits of improved sample efficiency via leveraging accuracy estimates from the partition function. Notably, PACED-RL achieves significantly faster training than GRPO and FlowRL. On HumanEval+, PACED-RL reaches the best performance achieved by GRPO and FlowRL using only  $0.49 \times$  and  $0.42 \times$  of their respective training time. Similarly, on LiveCodeBench, PACED-RL achieves the best performance of GRPO and FlowRL in  $0.67 \times$  and  $0.42 \times$  of the time.

Our results also indicate that for code generation tasks, adaptive prompt selection methods that utilize over-sampling question prompts, namely DS and LILO, are particularly ineffective. Unlike the mathematical reasoning domain, where fast rule-based verification is possible, the code generation domain requires slow execution-based verification (Wang et al., 2025a). The verification of increased number of code generations to estimate accuracies in the DS and the LILO setting leads to prohibitively slow training, leading to sub-optimal results.

**Mathematical Reasoning.** Results in Table 1 underscore the effectiveness of PACED-RL in the mathematical reasoning domain. Crucially, PACED-RL consistently outperforms GRPO and FlowRL by a wide margin. On the Qwen2.5-Math-7B model, PACED-RL improves over the performance of GRPO and FlowRL by 29.1% and 40.0% respectively on the AIME 24 benchmark, providing strong evidence of the effectiveness of our method. PACED-RL also consistently matches or exceeds the performance of

adaptive prompt selection baselines, despite not incorporating explicit auxiliary mechanisms for obtaining online accuracy estimates during training. This contrast is particularly notable given that PACED-RL does not incur significant compute overhead from rollout generation, as with DS and LILO. The improvement is most pronounced on the hardest AIME benchmarks: for instance, on AIME 25 with Qwen2.5-Math-7B, PACED-RL attains 13.1 compared to 11.7 for LILO, corresponding to an 11.9% relative gain.

**Diversity.** As a proxy for diversity, we assess the pass@ $k$  performance of PACED-RL. Achieving high pass@ $k$  requires the model to cover a broader space of plausible solution trajectories rather than concentrating probability mass on a single mode. Consequently, improvements in pass@ $k$ —particularly at larger  $k$ —are widely interpreted as evidence of increased solution diversity and exploration (Li et al., 2025b; Chen et al., 2025; Zhu et al., 2025b).

We compare the pass@ $k$  performance of PACED-RL compared to GRPO, FlowRL, and the untrained base models Qwen2.5-Math-1.5B and 7B. We evaluate on the AIME24/25 benchmarks, and generate using temperature set to 0.6 and a top- $p$  value of 0.95, following Yue et al. (2025). Fig. 3 shows that PACED-RL consistently outperforms baselines across values of  $k$ , with relative improvements over GRPO and FlowRL by up to 14.2% and 9.1% respectively. These results demonstrate the diversity-preserving nature and the superior exploration capability of PACED-RL.

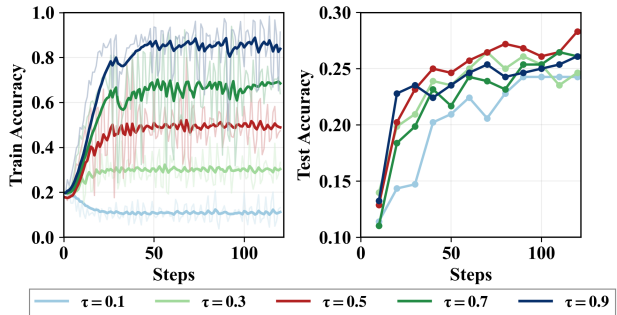


Figure 4. Train and test accuracies of Qwen2.5-Math-1.5B trained on the DeepScaleR dataset and evaluated on the MinervaMath benchmark, for target accuracy values  $\tau \in \{0.1, 0.3, 0.5, 0.7, 0.9\}$ .

### 5.3. Analysis

**Controlling Train Accuracy with the Partition Function.** Fig. 4 shows that our method selectively retains training questions whose estimated accuracies are close to  $\tau$ , thereby providing control over the training accuracy. Furthermore, our results reaffirm results from previous works (Foster et al., 2025; Gao et al., 2023) that maintaining questions with accuracies closest to 0.5 is optimal for sample-efficiency, achiev-

Model	Method	MATH-500	OlympiadBench	Minerva	AIME 24 Avg@32	AIME 25 Avg@32	Avg.↑	Avg. Rollouts↓
Qwen2.5-Math-1.5B	GRPO	70.6	34.2	24.2	10.3	6.3	29.1	<b>1.0</b> ×
	FlowRL	67.6	32.4	20.2	9.5	5.9	27.1	<b>1.0</b> ×
	DS	<u>72.8</u>	<u>36.8</u>	<u>28.3</u>	11.8	6.5	<u>31.2</u>	2.0×
	LILO	<u>73.2</u>	<u>36.2</u>	<u>27.9</u>	<u>12.0</u>	<u>6.9</u>	<u>31.2</u>	4.0×
Qwen2.5-Math-7B	MoPPS	71.6	36.6	26.1	11.4	6.6	30.4	<b>1.0</b> ×
	PACED-RL	<b>73.2</b>	<b>37.9</b>	<b>29.0</b>	<b>13.3</b>	<b>7.3</b>	<b>32.1</b>	<b>1.0</b> ×
	GRPO	77.6	39.7	<u>34.9</u>	23.9	10.3	37.2	<b>1.0</b> ×
	FlowRL	76.4	39.6	32.3	24.9	9.4	36.5	<b>1.0</b> ×
Qwen2.5-Math-7B	DS	<b>80.2</b>	44.0	34.5	26.6	12.0	<u>39.4</u>	2.5×
	LILO	78.4	<b>45.2</b>	<b>37.5</b>	<u>28.0</u>	11.7	<b>40.1</b>	4.0×
	MoPPS	<b>80.2</b>	42.2	34.1	24.0	<u>12.9</u>	38.6	<b>1.0</b> ×
	PACED-RL	80.0	<u>44.6</u>	34.1	<b>28.7</b>	<u>13.1</u>	<b>40.1</b>	<b>1.0</b> ×

Table 1. Pass@1(%) performance across mathematical reasoning benchmarks. We report Avg@32 performance for AIME benchmarks due to their small size. **Avg.** denotes the average of the performance on the 5 benchmarks. **Avg. Rollouts** denotes the average rollout count per step relative to GRPO, expressed as a multiplicative factor. Best results are in **bold**. Second best results are underlined.

ing the highest test accuracy throughout training. Setting  $\tau = 0.9$  yields the fastest *initial* gains in test accuracy but quickly plateaus, ultimately resulting in sub-optimal performance. Moreover, the run with  $\tau = 0.1$  produces the weakest results overall, with test accuracy consistently trailing all other settings throughout training. Taken together, these results indicate that by restricting training to an effective level of difficulty, adaptive prompt selection makes policy learning robust to dataset difficulty, enabling efficient and stable improvement on datasets of any difficulty via a sustained focus on the most informative question prompts.

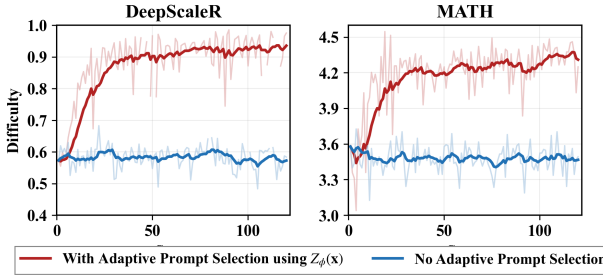


Figure 5. Progression of the average difficulty of question prompts sampled in each training batch under the Qwen2.5-Math-7B model.

### Progression of Question Difficulty During Training.

Figure 5 shows the evolution of the mean difficulty of sampled question prompts over the course of training. For the MATH dataset, we utilize the human-annotated difficulty labels, which range from level 1, indicating the simplest questions, to level 5, indicating the most complex questions. For DeepScaleR, which does not have human-annotated difficulty labels, we use the difficulty labels from Shi et al. (2025), defined as 1 - pass@1 accuracy computed over all questions using the Qwen2.5-Math-7B model. Without adaptive prompt selection, the mean difficulty remains con-

stant throughout training. However, with adaptive prompt selection guided by partition function-guided accuracy estimates, the mean difficulties progressively increase, shifting toward harder questions as the model improves. This trend is expected, as a question regarded as having intermediate difficulty in earlier parts of training is likely to become easier for the policy as training progresses.

**Ablation on the Replay Buffer.** To isolate the contribution of our accuracy estimate error-prioritized replay mechanism, we conduct an ablation study on the replay strategy in Table 2. Incorporating replay yields consistent performance improvements across all mathematical reasoning benchmarks, indicating that selectively revisiting question-output pairs whose predicted accuracy disagrees largely with observed accuracy provides an informative training signal for improving sample efficiency.

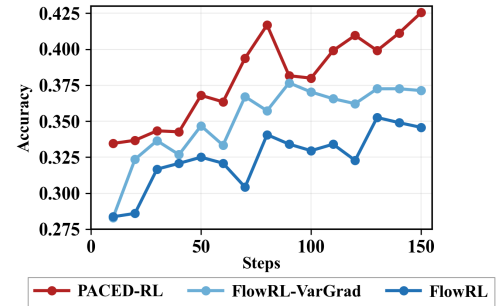


Figure 6. Progression of average test accuracy of FlowRL, FlowRL-VarGrad, and PACED-RL across the 5 mathematical reasoning benchmarks. Results obtained using Qwen2.5-Math-1.5B trained on the DeepScaleR dataset.

**Comparison to TB-VarGrad.** To stabilize training by circumventing the need to train the partition function, several

Model	Method	MATH-500	Olympiad	Minerva	AIME 24 Avg@32	AIME 25 Avg@32	Avg.
Qwen2.5-Math-1.5B	PACED-RL	73.2	37.9	29.0	13.3	7.3	32.1
	w/o Replay	73.0	36.3	26.1	9.8	6.1	30.2

Table 2. Ablation study on the accuracy estimate error-prioritized replay, using Qwen2.5-Math-1.5B. Results show the pass@1(%) performance across the mathematical reasoning benchmarks. Using the replay mechanism increases performance across all benchmarks.

Model	$Z_\phi(\mathbf{x})$	Computation (s)	Total (s)
Qwen2.5-Math-1.5B	0.035	308	
Qwen2.5-Math-7B	0.110	370	
DS-Distill-1.5B	0.020	1086	

Table 3. Comparison between the average time taken for the computation of  $Z_\phi(\mathbf{x})$  for all question prompts in the dataset and the average total time taken per step. DS-Distill-1.5B denotes the DeepSeek-R1-Distill-Qwen-1.5B model.

prior works (Zhang et al., 2023; Venkatraman et al., 2024; Bartoldson et al., 2025) adopt the VarGrad variant of the Trajectory Balance objective, which replaces the learned partition function  $Z_\phi(\mathbf{x})$  with a batch-level estimate. Specifically, for a prompt  $\mathbf{x}_i$  and its  $N$  corresponding rollouts  $\{\mathbf{y}_{i,j}\}_{j=1}^N$ , the batch estimate of  $Z_\phi(\mathbf{x}_i)$  can be obtained as:

$$\log \hat{Z}(\mathbf{x}_i) = \frac{1}{N} \sum_{j=1}^N (R(\mathbf{x}_i, \mathbf{y}_{i,j}) - \log \pi_\theta(\mathbf{y}_{i,j} \mid \mathbf{x}_i)). \quad (10)$$

Using the Qwen2.5-Math-1.5B model, we compare PACED-RL against FlowRL-VarGrad, a variant of FlowRL that uses the batch-estimate  $Z_\phi(\mathbf{x})$  for training instead of learning the partition function. Consistent with the observations of Zhang et al. (2023), Fig. 6 shows that FlowRL-VarGrad converges faster and achieves higher test performance than the original FlowRL approach. Nevertheless, PACED-RL consistently outperforms FlowRL-VarGrad throughout training, demonstrating that explicitly learning the partition function—and leveraging the accuracy information it encodes for increased sample efficiency—is more effective than relying on a batch-estimate approximation. Note that as the estimate in Eq. 10 can only be made *after* the rollout phase, it cannot be used as a lightweight online accuracy estimator.

**Computational Overhead.** Due to the small size of the 3-layer MLP used to parameterize  $Z_\phi$ , the computation of  $Z_\phi$  for all question prompts in the dataset can be efficiently performed using large-batch inference. To illustrate the negligible computational wall-clock time overhead associated with evaluating the partition function, we report in Table 3 the average time required to compute  $Z_\phi(\mathbf{x})$  to obtain  $\{\hat{p}_{\text{old}}(\mathbf{x}_i)\}_{i=1}^{|\mathcal{D}|}$  alongside the average total runtime per training step. Across all models, the time taken for obtaining

$Z_\phi(\mathbf{x})$  values is several orders of magnitude smaller than the total per-step computation time. By exploiting these low-cost accuracy estimates obtainable with minimal additional latency, PACED-RL substantially improves sample efficiency, translating into notable performance gains.

## 6. Conclusion & Future Works

**Conclusion.** We introduce PACED-RL, a distribution-matching post-training framework that improves LLM reasoning by explicitly leveraging the learned partition function as an online accuracy signal. By exploiting the accuracy signals obtained without incurring additional compute cost, PACED-RL adaptively concentrates training on the most informative training samples, leading to more effective and sample-efficient policy learning for LLM reasoning. Extensive experiments on mathematical reasoning and code generation tasks across three models demonstrate the consistent effectiveness of our proposed approach. Overall, PACED-RL offers a principled and a scalable pathway towards a more efficient distribution-matching methods for enhancing the reasoning capabilities of LLMs.

**Future Works** The interpretation of the partition function as an online accuracy estimator opens up new opportunities for inference time strategies. Beyond its role in training, future work could investigate techniques such as adaptive self-consistency, where additional samples are selectively allocated to question prompts predicted to be difficult according to the learned partition function, enabling more compute-efficient and accuracy-aware reasoning.

Additionally, we leave the study of applying GFlowNet objective variants—such as Detailed Balance (Bengio et al., 2023) and Sub-Trajectory Balance (Madan et al., 2023)—to PACED-RL in multi-step reasoning settings for future work. This extension would allow us to transition from leveraging the partition function as a question-level difficulty estimator to utilizing intermediate state *flows* as step-level difficulty signals, thereby enabling more granular credit assignment and difficulty-aware guidance in multi-step reasoning tasks.

Lastly, a promising direction for future works is to extend PACED-RL to asynchronous GFlowNet reinforcement learning frameworks (Bartoldson et al., 2025) to substantially improve scalability and training throughput.

## Impact Statement

This paper presents work whose goal is to advance the field of Machine Learning. We confirm that all datasets included in our study are sourced from established, publicly available repositories and standard benchmarks. There are many potential societal consequences of our work, none which we feel must be specifically highlighted here.

## References

Achiam, J., Held, D., Tamar, A., and Abbeel, P. Constrained policy optimization. In *International conference on machine learning*, pp. 22–31. PMLR, 2017.

Bae, S., Hong, J., Lee, M. Y., Kim, H., Nam, J., and Kwak, D. Online difficulty filtering for reasoning oriented reinforcement learning. *arXiv preprint arXiv:2504.03380*, 2025.

Bartoldson, B. R., Venkatraman, S., Diffenderfer, J., Jain, M., Ben-Nun, T., Lee, S., Kim, M., Obando-Ceron, J., Bengio, Y., and Kailkhura, B. Trajectory balance with asynchrony: Decoupling exploration and learning for fast, scalable LLM post-training. In *The Thirty-ninth Annual Conference on Neural Information Processing Systems*, 2025. URL <https://openreview.net/forum?id=VwPt1WDQNB>.

Bengio, Y., Lahlou, S., Deleu, T., Hu, E. J., Tiwari, M., and Bengio, E. Gflownet foundations. *Journal of Machine Learning Research*, 24(210):1–55, 2023.

Chen, M. Evaluating large language models trained on code. *arXiv preprint arXiv:2107.03374*, 2021.

Chen, Z., Qin, X., Wu, Y., Ling, Y., Ye, Q., Zhao, W. X., and Shi, G. Pass@ k training for adaptively balancing exploration and exploitation of large reasoning models. *arXiv preprint arXiv:2508.10751*, 2025.

Comanici, G., Bieber, E., Schaeckermann, M., Pasupat, I., Sachdeva, N., Dhillon, I., Blistein, M., Ram, O., Zhang, D., Rosen, E., et al. Gemini 2.5: Pushing the frontier with advanced reasoning, multimodality, long context, and next generation agentic capabilities. *arXiv preprint arXiv:2507.06261*, 2025.

Fedus, W., Ramachandran, P., Agarwal, R., Bengio, Y., Larochelle, H., Rowland, M., and Dabney, W. Revisiting fundamentals of experience replay. In *International conference on machine learning*, pp. 3061–3071. PMLR, 2020.

Foster, T., Sims, A., Forkel, J., and Foerster, J. N. LILO: Learning to reason at the frontier of learnability. In *The Thirty-ninth Annual Conference on Neural Information Processing Systems*, 2025. URL <https://openreview.net/forum?id=8HYeWMf0W3>.

Gao, L., Schulman, J., and Hilton, J. Scaling laws for reward model overoptimization. In *International Conference on Machine Learning*, pp. 10835–10866. PMLR, 2023.

Guo, D., Yang, D., Zhang, H., Song, J., Zhang, R., Xu, R., Zhu, Q., Ma, S., Wang, P., Bi, X., et al. Deepseek-r1: Incentivizing reasoning capability in llms via reinforcement learning. *arXiv preprint arXiv:2501.12948*, 2025.

He, C., Luo, R., Bai, Y., Hu, S., Thai, Z., Shen, J., Hu, J., Han, X., Huang, Y., Zhang, Y., et al. Olympiadbench: A challenging benchmark for promoting agi with olympiad-level bilingual multimodal scientific problems. In *Proceedings of the 62nd Annual Meeting of the Association for Computational Linguistics (Volume 1: Long Papers)*, pp. 3828–3850, 2024.

Hendrycks, D., Burns, C., Kadavath, S., Arora, A., Basart, S., Tang, E., Song, D., and Steinhardt, J. Measuring mathematical problem solving with the MATH dataset. In *Thirty-fifth Conference on Neural Information Processing Systems Datasets and Benchmarks Track (Round 2)*, 2021. URL <https://openreview.net/forum?id=7Bywt2mQsCe>.

Hessel, M., Modayil, J., Van Hasselt, H., Schaul, T., Os-trovski, G., Dabney, W., Horgan, D., Piot, B., Azar, M., and Silver, D. Rainbow: Combining improvements in deep reinforcement learning. In *Proceedings of the AAAI conference on artificial intelligence*, volume 32, 2018.

Horgan, D., Quan, J., Budden, D., Barth-Maron, G., Hessel, M., van Hasselt, H., and Silver, D. Distributed prioritized experience replay. In *International Conference on Learning Representations*, 2018. URL <https://openreview.net/forum?id=H1Dy---0Z>.

Huang, A., Block, A., Foster, D. J., Rohatgi, D., Zhang, C., Simchowitz, M., Ash, J. T., and Krishnamurthy, A. Self-improvement in language models: The sharpening mechanism. In *The Thirteenth International Conference on Learning Representations*, 2025. URL <https://openreview.net/forum?id=WJaUkwci9o>.

Jaech, A., Kalai, A., Lerer, A., Richardson, A., El-Kishky, A., Low, A., Helyar, A., Madry, A., Beutel, A., Carney, A., et al. Openai o1 system card. *arXiv preprint arXiv:2412.16720*, 2024.

Jain, N., Han, K., Gu, A., Li, W.-D., Yan, F., Zhang, T., Wang, S., Solar-Lezama, A., Sen, K., and Stoica, I. Livecodebench: Holistic and contamination free evaluation of large language models for code. In *The Thirteenth*

*International Conference on Learning Representations*, 2025. URL <https://openreview.net/forum?id=chfJJYC3iL>.

Kim, M., Yun, T., Bengio, E., Zhang, D., Bengio, Y., Ahn, S., and Park, J. Local search GFlownets. In *The Twelfth International Conference on Learning Representations*, 2024. URL <https://openreview.net/forum?id=6cFcw1Rxww>.

Kwon, O. J., Matsunaga, D., and Kim, K.-E. Gdpo: Learning to directly align language models with diversity using gflownets. In *Proceedings of the 2024 Conference on Empirical Methods in Natural Language Processing*, pp. 17120–17139, 2024.

Lee, S., Kim, M., Cherif, L., Dobre, D., Lee, J., Hwang, S. J., Kawaguchi, K., Gidel, G., Bengio, Y., Malkin, N., and Jain, M. Learning diverse attacks on large language models for robust red-teaming and safety tuning. In *The Thirteenth International Conference on Learning Representations*, 2025. URL <https://openreview.net/forum?id=1mXufFuv95>.

Lewkowycz, A., Andreassen, A., Dohan, D., Dyer, E., Michalewski, H., Ramasesh, V., Sloane, A., Anil, C., Schlag, I., Gutman-Solo, T., et al. Solving quantitative reasoning problems with language models. *Advances in neural information processing systems*, 35:3843–3857, 2022.

Li, S., Zhou, Z., Lam, W., Yang, C., and Lu, C. Repo: Replay-enhanced policy optimization. *arXiv preprint arXiv:2506.09340*, 2025a.

Li, T., Zhang, Y., Yu, P., Saha, S., Khashabi, D., Weston, J., Lanchantin, J., and Wang, T. Jointly reinforcing diversity and quality in language model generations. *arXiv preprint arXiv:2509.02534*, 2025b.

Li, Z., Chen, C., Xu, T., Qin, Z., Xiao, J., Luo, Z.-Q., and Sun, R. Preserving diversity in supervised fine-tuning of large language models. In *The Thirteenth International Conference on Learning Representations*, 2025c. URL <https://openreview.net/forum?id=NQEe7B7bSw>.

Luo, M., Tan, S., Huang, R., Patel, A., Ariyak, A., Wu, Q., Shi, X., Xin, R., Cai, C., Weber, M., et al. Deepcoder: A fully open-source 14b coder at o3-mini level. *Notion Blog*, 2025a.

Luo, M., Tan, S., Wong, J., Shi, X., Tang, W. Y., Roongta, M., Cai, C., Luo, J., Zhang, T., Li, L. E., et al. Deepscaler: Surpassing o1-preview with a 1.5 b model by scaling rl. *Notion Blog*, 2025b.

Madan, K., Rector-Brooks, J., Korablyov, M., Bengio, E., Jain, M., Nica, A. C., Bosc, T., Bengio, Y., and Malkin, N. Learning gflownets from partial episodes for improved convergence and stability. In *International Conference on Machine Learning*, pp. 23467–23483. PMLR, 2023.

Malkin, N., Jain, M., Bengio, E., Sun, C., and Bengio, Y. Trajectory balance: Improved credit assignment in gflownets. *Advances in Neural Information Processing Systems*, 35:5955–5967, 2022.

Martens, J. New insights and perspectives on the natural gradient method. *Journal of Machine Learning Research*, 21(146):1–76, 2020.

Padmakumar, V. and He, H. Does writing with language models reduce content diversity? In *The Twelfth International Conference on Learning Representations*, 2024. URL <https://openreview.net/forum?id=Feiz5HtCD0>.

Qu, Y., Wang, Q., Mao, Y., Hu, V. T., Ommer, B., and Ji, X. Can prompt difficulty be online predicted for accelerating rl finetuning of reasoning models? *arXiv preprint arXiv:2507.04632*, 2025.

Schaul, T., Quan, J., Antonoglou, I., and Silver, D. Prioritized experience replay. *arXiv preprint arXiv:1511.05952*, 2015.

Schulman, J., Levine, S., Abbeel, P., Jordan, M., and Moritz, P. Trust region policy optimization. In *International conference on machine learning*, pp. 1889–1897. PMLR, 2015.

Schulman, J., Wolski, F., Dhariwal, P., Radford, A., and Klimov, O. Proximal policy optimization algorithms. *arXiv preprint arXiv:1707.06347*, 2017.

Shao, Z., Wang, P., Zhu, Q., Xu, R., Song, J., Bi, X., Zhang, H., Zhang, M., Li, Y., et al. Deepseekmath: Pushing the limits of mathematical reasoning in open language models. *arXiv preprint arXiv:2402.03300*, 2024.

Shen, M. W., Bengio, E., Hajiramezanali, E., Loukas, A., Cho, K., and Biancalani, T. Towards understanding and improving gflownet training. In *International conference on machine learning*, pp. 30956–30975. PMLR, 2023.

Sheng, G., Zhang, C., Ye, Z., Wu, X., Zhang, W., Zhang, R., Peng, Y., Lin, H., and Wu, C. Hybridflow: A flexible and efficient rlhf framework. In *Proceedings of the Twentieth European Conference on Computer Systems*, pp. 1279–1297, 2025.

Shi, T., Wu, Y., Song, L., Zhou, T., and Zhao, J. Efficient reinforcement finetuning via adaptive curriculum learning, 2025. URL <https://arxiv.org/abs/2504.05520>.

Shypula, A., Li, S., Zhang, B., Padmakumar, V., Yin, K., and Bastani, O. Evaluating the diversity and quality of LLM generated content. In *Second Conference on Language Modeling*, 2025. URL <https://openreview.net/forum?id=O7bF6nlSOD>.

Sujit, S., Nath, S., Braga, P., and Ebrahimi Kahou, S. Prioritizing samples in reinforcement learning with reducible loss. *Advances in Neural Information Processing Systems*, 36:23237–23258, 2023.

Venkatraman, S., Jain, M., Scimeca, L., Kim, M., Sendera, M., Hasan, M., Rowe, L., Mittal, S., Lemos, P., Bengio, E., et al. Amortizing intractable inference in diffusion models for vision, language, and control. *Advances in neural information processing systems*, 37:76080–76114, 2024.

Wang, B., Lee, C., Lee, N., Lin, S.-C., Dai, W., Chen, Y., Chen, Y., Yang, Z., Liu, Z., Shoeybi, M., et al. Nemotron-cascade: Scaling cascaded reinforcement learning for general-purpose reasoning models. *arXiv preprint arXiv:2512.13607*, 2025a.

Wang, C., Wei, L., Zhang, Y., Shao, C., Dan, Z., Huang, W., Wang, Y., and Zhang, Y. Eframe: Deeper reasoning via exploration-filtering-replay reinforcement learning framework. *arXiv preprint arXiv:2506.22200*, 2025b.

Yang, A., Zhang, B., Hui, B., Gao, B., Yu, B., Li, C., Liu, D., Tu, J., Zhou, J., Lin, J., et al. Qwen2. 5-math technical report: Toward mathematical expert model via self-improvement. *arXiv preprint arXiv:2409.12122*, 2024.

Yu, F., Jiang, L., Kang, H., Hao, S., and Qin, L. Flow of reasoning: Training LLMs for divergent reasoning with minimal examples. In *Forty-second International Conference on Machine Learning*, 2025a. URL <https://openreview.net/forum?id=qyMxunrR2j>.

Yu, Q., Zhang, Z., Zhu, R., Yuan, Y., Zuo, X., Yue, Y., Dai, W., Fan, T., Liu, G., Liu, L., et al. Dapo: An open-source llm reinforcement learning system at scale. *arXiv preprint arXiv:2503.14476*, 2025b.

Yue, Y., Chen, Z., Lu, R., Zhao, A., Wang, Z., Yue, Y., Song, S., and Huang, G. Does reinforcement learning really incentivize reasoning capacity in LLMs beyond the base model? In *The Thirty-ninth Annual Conference on Neural Information Processing Systems*, 2025. URL <https://openreview.net/forum?id=40sgYD7em5>.

Zeng, Y., Sun, Z., Ji, B., Min, E., Cai, H., Wang, S., Yin, D., Zhang, H., Chen, X., and Wang, J. Cures: From gradient analysis to efficient curriculum learning for reasoning llms. *arXiv preprint arXiv:2510.01037*, 2025.

Zhang, D. W., Rainone, C., Peschl, M., and Bondesan, R. Robust scheduling with gflownets. In *ICLR*, 2023.

Zhang, E., Yan, X., Lin, W., Zhang, T., and Qianchun, L. Learning like humans: Advancing llm reasoning capabilities via adaptive difficulty curriculum learning and expert-guided self-reformulation. In *Proceedings of the 2025 Conference on Empirical Methods in Natural Language Processing*, pp. 6630–6644, 2025.

Zheng, H., Zhou, Y., Bartoldson, B. R., Kailkhura, B., Lai, F., Zhao, J., and Chen, B. Act only when it pays: Efficient reinforcement learning for LLM reasoning via selective rollouts. In *The Thirty-ninth Annual Conference on Neural Information Processing Systems*, 2025. URL <https://openreview.net/forum?id=x51ITYXmW2>.

Zhu, X., Cheng, D., Zhang, D., Li, H., Zhang, K., Jiang, C., Sun, Y., Hua, E., Zuo, Y., Lv, X., et al. Flowrl: Matching reward distributions for llm reasoning. *arXiv preprint arXiv:2509.15207*, 2025a.

Zhu, X., Xia, M., Wei, Z., Chen, W.-L., Chen, D., and Meng, Y. The surprising effectiveness of negative reinforcement in LLM reasoning. In *The Thirty-ninth Annual Conference on Neural Information Processing Systems*, 2025b. URL <https://openreview.net/forum?id=ftV1LG9cks>.

## A. Derivations

### A.1. Proof of Proposition 4.1

For a fixed question  $\mathbf{x}$ , and rollouts from  $\pi_{\text{old}}(\cdot | \mathbf{x})$ , the expected loss is

$$\mathcal{L}(\mathbf{x}) := \mathbb{E}_{\mathbf{y} \sim \pi_{\text{old}}(\cdot | \mathbf{x})} \left[ \left( \log \frac{Z_\phi(\mathbf{x}) \pi_\theta(\mathbf{y} | \mathbf{x})}{\pi_{\text{old}}(\mathbf{y} | \mathbf{x}) \exp(\beta^{-1} r(\mathbf{x}, \mathbf{y}))} \right)^2 \right]. \quad (11)$$

By differentiating w.r.t.  $\log Z_\phi(\mathbf{x})$ , we have

$$\frac{\partial \mathcal{L}(\mathbf{x})}{\partial \log Z_\phi(\mathbf{x})} = \mathbb{E}_{\mathbf{y} \sim \pi_{\text{old}}(\cdot | \mathbf{x})} [2 (\log Z_\phi(\mathbf{x}) + \log \pi_\theta(\mathbf{y} | \mathbf{x}) - \log \pi_{\text{old}}(\mathbf{y} | \mathbf{x}) - \beta^{-1} r(\mathbf{x}, \mathbf{y}))]. \quad (12)$$

Setting the derivative to zero yields

$$\mathbb{E}_{\mathbf{y} \sim \pi_{\text{old}}(\cdot | \mathbf{x})} [\log Z^*(\mathbf{x}) + \log \pi_\theta(\mathbf{y} | \mathbf{x}) - \log \pi_{\text{old}}(\mathbf{y} | \mathbf{x}) - \beta^{-1} r(\mathbf{x}, \mathbf{y})] = 0, \quad (13)$$

hence

$$\log Z^*(\mathbf{x}) = \mathbb{E}_{\mathbf{y} \sim \pi_{\text{old}}(\cdot | \mathbf{x})} [\beta^{-1} r(\mathbf{x}, \mathbf{y}) + \log \pi_{\text{old}}(\mathbf{y} | \mathbf{x}) - \log \pi_\theta(\mathbf{y} | \mathbf{x})]. \quad (14)$$

By rearranging, we have

$$\mathbb{E}_{\mathbf{y} \sim \pi_{\text{old}}(\cdot | \mathbf{x})} [r(\mathbf{x}, \mathbf{y})] = \beta \log Z^*(\mathbf{x}) - \beta \mathbb{E}_{\mathbf{y} \sim \pi_{\text{old}}(\cdot | \mathbf{x})} [\log \pi_{\text{old}}(\mathbf{y} | \mathbf{x}) - \log \pi_\theta(\mathbf{y} | \mathbf{x})] \quad (15)$$

$$= \beta \log Z^*(\mathbf{x}) - \beta D_{\text{KL}}(\pi_{\text{old}}(\cdot | \mathbf{x}) \parallel \pi_\theta(\cdot | \mathbf{x})). \quad (16)$$

Since reward is 0 for a wrong rollout and 1 for a correct rollout, we have

$$p_{\text{old}}(\mathbf{x}) = \mathbb{E}_{\mathbf{y} \sim \pi_{\text{old}}(\cdot | \mathbf{x})} [r(\mathbf{x}, \mathbf{y})]. \quad (17)$$

Substituting Eq. 17 to Eq. 16 yields

$$p_{\text{old}}(\mathbf{x}) = \beta \log Z^*(\mathbf{x}) - \beta D_{\text{KL}}(\pi_{\text{old}}(\cdot | \mathbf{x}) \parallel \pi_\theta(\cdot | \mathbf{x})). \quad (18)$$

### A.2. Generalizing to Arbitrary Binary Reward Configurations

Rather than assigning a reward value of 0 to an incorrect output and 1 to a correct output, several prior works adopt alternative reward configurations. For example, DAPO (Yu et al., 2025b) assigns a reward of -1 to incorrect outputs and a reward of 1 to correct outputs. We show that the relationship between the partition function and accuracy estimates extends naturally to arbitrary reward configurations.

Assume that a reward value of  $a$  is assigned to an incorrect output and a reward value of  $b$  is assigned to a correct output, where  $b \neq a$ . Then, we can express  $\mathbb{E}_{\mathbf{y} \sim \pi_{\text{old}}(\cdot | \mathbf{x})} [r(\mathbf{x}, \mathbf{y})]$  as follows:

$$\mathbb{E}_{\mathbf{y} \sim \pi_{\text{old}}(\cdot | \mathbf{x})} [r(\mathbf{x}, \mathbf{y})] = a (1 - p_{\text{old}}(\mathbf{x})) + b p_{\text{old}}(\mathbf{x}) \quad (19)$$

$$= a + (b - a) p_{\text{old}}(\mathbf{x}). \quad (20)$$

Expressing in terms of  $p_{\text{old}}(\mathbf{x})$  gives

$$p_{\text{old}}(\mathbf{x}) = \frac{\mathbb{E}_{\mathbf{y} \sim \pi_{\text{old}}(\cdot | \mathbf{x})} [r(\mathbf{x}, \mathbf{y})] - a}{b - a}. \quad (21)$$

Substituting Eq. (16) into Eq. (21) yields

$$p_{\text{old}}(\mathbf{x}) = \frac{\beta \log Z^*(\mathbf{x}) - \beta D_{\text{KL}}(\pi_{\text{old}}(\cdot | \mathbf{x}) \parallel \pi_\theta(\cdot | \mathbf{x})) - a}{b - a}. \quad (22)$$

Note that setting  $a = 0$  and  $b = 1$  recovers the result obtained in Eq. 18.

Hyperparameter	DeepScaleR	DeepCoder
Learning Rate (LR)	$1 \times 10^{-6}$	$1 \times 10^{-6}$
Gradient Clip	1.0	1.0
Optimizer	AdamW	AdamW
Weight Decay	0.1	0.1
Warm-up Steps	10	10
Global Batch Size	128	64
PPO Mini-batch Size	32	32
Micro-batch Size (per GPU)	8	8
Rollouts per Question ( $N$ )	8	8
Clip Ratio	0.2	0.2
KL Divergence Penalty	0.0	0.0
Entropy Coefficient	0.0	0.0
Rollout Temperature	1.0	1.0
Max Input Tokens	1024	1024
Max Response Tokens	3072	3072

Table 4. Hyperparameters used for training on the DeepScaleR and DeepCoder datasets. Unspecified hyperparameters inherit the default configurations under the verl library.

---

**Algorithm 1** PACED-RL

**Require:** dataset  $\mathcal{D}$ ; steps  $T$ ; batch size  $m$ ; rollout size  $N$ ; KL coefficient  $\beta$ ; target accuracy  $\tau$ ; buffer capacity  $B_{\max}$ ; replay add count  $B_{\text{add}}$

- 1: Initialize policy  $\pi_0$  and partition network  $Z_\phi$
- 2: Initialize replay buffer  $\mathcal{B} \leftarrow \emptyset$  with capacity  $B_{\max}$
- 3: Set  $\pi_{\text{old}} \leftarrow \pi_0$
- 4: **for**  $t = 0$  **to**  $T - 1$  **do**
- 5:   Estimate accuracies:  $\hat{p}_{\text{old}}(\mathbf{x}) \leftarrow \beta \log Z_\phi(\mathbf{x}) \quad \forall \mathbf{x} \in \mathcal{D}$
- 6:   Select  $m$  questions from accuracy estimates:  $\mathcal{D}_t \leftarrow \underset{|\mathcal{D}_t|=m}{\operatorname{argmin}} \sum_{\mathbf{x} \in \mathcal{D}_t} |\hat{p}_{\text{old}}(\mathbf{x}) - \tau|$
- 7:   Generate trajectories using  $\pi_{\text{old}}$ :  $\mathcal{T}_t \leftarrow \{(\mathbf{x}_i, \{\mathbf{y}_{i,j}\}_{j=1}^N)\}_{i=1}^m, \quad \mathbf{y}_{i,j} \sim \pi_{\text{old}}(\cdot | \mathbf{x}_i)$
- 8:   Augment training batch with replay:  $\tilde{\mathcal{T}}_t \leftarrow \mathcal{T}_t \cup \mathcal{B}$
- 9:   Update  $\pi_t$  to  $\pi_{t+1}$ , update  $Z_\phi$  on  $\tilde{\mathcal{T}}_t$  using Eq. (6)
- 10:   Set  $\pi_{\text{old}} \leftarrow \pi_{t+1}$
- 11:   Filter out incorrect trajectories from  $\mathcal{T}_t$ :  $\mathcal{T}'_t \leftarrow \{(\mathbf{x}, \{\mathbf{y}_j\}) \in \mathcal{T}_t \mid r(\mathbf{x}, \mathbf{y}_j) = 1\}$
- 12:   Select  $B_{\text{add}}$  samples from  $\mathcal{T}'_t$  to add to buffer:  $\mathcal{C}_t \leftarrow \underset{\mathcal{C}_t \subseteq \mathcal{T}'_t, |\mathcal{C}_t|=B_{\text{add}}}{\operatorname{argmax}} \sum_{(\mathbf{x}, \{\mathbf{y}_j\}) \in \mathcal{C}_t} |p_{\text{old}}(\mathbf{x}) - \hat{p}_{\text{old}}(\mathbf{x})|$
- 13:   Add replay candidates to buffer:  $\mathcal{B} \leftarrow \text{Push}(\mathcal{B}, \mathcal{C}_t)$
- 14: **end for**

---

## B. Experimental Details

### B.1. Additional Training Details

For training on Qwen2.5-Math-1.5B and Deepseek-Distill-Qwen-1.5B models, we use a single node consisting of 2 A6000 GPUs. For training on the Qwen2.5-Math-7B model, we use a single node consisting of 4 A100 GPUs. We use the verl (Sheng et al., 2025) library for training and evalution across all runs. For all runs in the mathematical reasoning domain, we use a training budget of 150 steps. For runs on the code generation task, due to the substantial time required for training, we limit the training to 40 hours. As for the training and evaluation data, we follow the preprocessing pipeline from the official FlowRL repository<sup>1</sup>. Other training hyperparameters kept constant across all runs are listed in Table 4.

### B.2. PACED-RL Implementation Details

For the partition function  $Z_\phi(\mathbf{x})$ , following (Lee et al., 2025; Zhu et al., 2025a), we use a 3-layer MLP on top of LLM last hidden layer embeddings. We use the last hidden layer embeddings of the frozen base model as the input to the  $Z_\phi(\mathbf{x})$ . The

<sup>1</sup><https://github.com/Xuekai-Zhu/FlowRL>

$Z_\phi(\mathbf{x})$  module is optimized using a separate PyTorch optimizer, with the learning rate set to 1e-4. Lastly, after obtaining the accuracy estimates from Eq. 8, we clip the value to [0,1].

### B.3. Baseline Implementation Details

For GRPO (Shao et al., 2024) and DS (Yu et al., 2025b), we use the implementation provided in the verl (Sheng et al., 2025) library. For FlowRL (Zhu et al., 2025a) and MoPPS (Qu et al., 2025), we adopt the official implementations and default hyperparameters provided by the authors in their implementations. For LILO (Foster et al., 2025), we implement the over-sampling and rejection-sampling procedure that selects the top- $m$  question prompts whose accuracies are closest to 0.5. Following the original specification, at each training step we uniformly sample  $4m$  prompts from the dataset and generate  $N$  rollouts for each prompt. The  $m$  prompts whose empirical accuracies are closest to 0.5 are then selected for training, and the corresponding rollouts are reused for policy optimization.

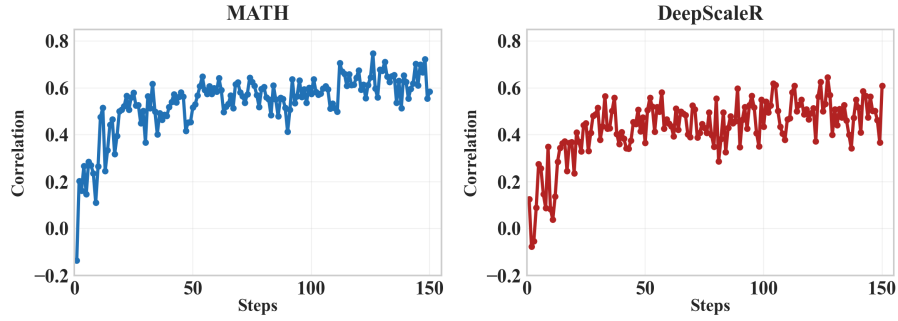


Figure 7. Spearman’s correlation coefficient measured on the MATH training data and the DeepScaleR training data, using the Qwen2.5-Math-1.5B model.

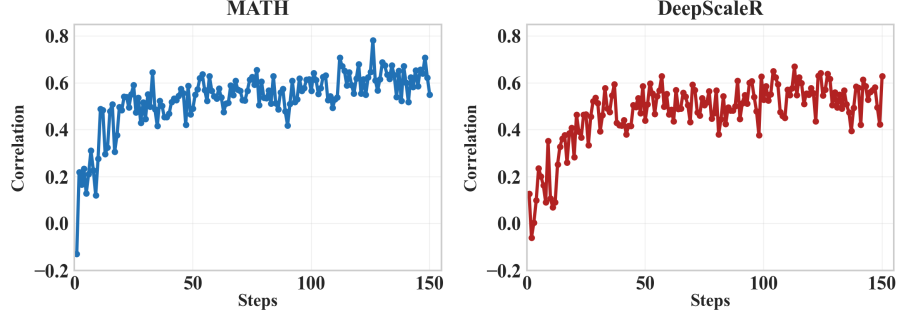


Figure 8. Pearson’s correlation coefficient measured on the MATH training data and the DeepScaleR training data, using the Qwen2.5-Math-1.5B model..

## C. Supplementary Results

### C.1. Correlation of Accuracy Estimates to Empirically Observed Accuracies

Fig. 7 and Fig. 8 show the Spearman’s correlation coefficient and Pearson’s correlation coefficient for randomly sampled question prompts over the training process, on the Qwen2.5-Math-1.5B model. The constantly high ( $> 0.5$ ) correlation values after  $\sim 20$  training steps indicate that the online accuracy estimates from  $Z_\phi$  serve as reliable estimators.

## D. Future Works

The interpretation of the partition function as an online accuracy estimator opens up new opportunities for inference time strategies. Beyond its role in training, future work could investigate techniques such as adaptive self-consistency, where additional samples are selectively allocated to question prompts predicted to be difficult according to the learned partition

function, enabling more compute-efficient and accuracy-aware reasoning.

Additionally, a promising direction for future work is to extend PACED-RL to fully asynchronous reinforcement learning frameworks. While the TB objective naturally admits off-policy data—already leveraged in this work through accuracy-estimate–error–prioritized replay—our current implementation remains synchronous. Fully exploiting the off-policy capability of TB by decoupling rollout generation from policy optimization (Bartoldson et al., 2025), could substantially improve scalability and training throughput

## E. Limitations

While we evaluate PACED-RL on models with 1.5B and 7B parameters and observe consistent improvements across both scales, we do not explore substantially larger models due to computational constraints. As a result, it remains an open question whether the gains of PACED-RL persist when applied to substantially larger LLMs.

In addition, although our experiments span both mathematical reasoning and code generation tasks, we focus exclusively on domains where verifiable reward signals are available. We do not study non-verifiable settings such as preference optimization or open-ended creative generation. Extending PACED-RL to these domains may require more sophisticated reward modeling or alternative accuracy estimation mechanisms, which we leave to future work.

Lastly, our low-cost accuracy estimation based on the learned partition function  $Z_\phi$  relies on the assumption that the term  $\beta D_{\text{KL}}(\pi_{\text{old}}(\cdot | \mathbf{x}) \| \pi_\theta(\cdot | \mathbf{x}))$  remains sufficiently small during training and can therefore be safely neglected. While our empirical results demonstrate that PACED-RL yields consistent performance improvements in both code generation and mathematical reasoning domains, the validity of this assumption may depend on the characteristics of the task and training dynamics. In particular, when extending PACED-RL to other domains, this approximation should be carefully examined, as deviations from this regime could degrade the accuracy of the estimator. We leave a systematic investigation of this assumption across broader domains to future work.